

Doping dependence of the exchange energies in bilayer manganites: Role of orbital degrees of freedom

G. Jackeli^{1*}, N.B. Perkins^{2,3}

¹*Centre de Recherches sur les Très Basses Températures, Laboratoire Associé à l'Université Joseph Fourier, Centre National de la Recherche Scientifique, BP 166, 38042, Grenoble Cédex 9, France*

²*Joint Institute for Nuclear Research, Dubna, Moscow region, 141980, Russia*

³*Max-Planck-Institut für Physik komplexer Systeme, Nöthnitzer Str. 38 01187 Dresden, Germany.*

Recently, an intriguing doping dependence of the exchange energies in the bilayer manganites $\text{La}_{2-2x}\text{Sr}_{1+2x}\text{Mn}_2\text{O}_7$ has been observed in the neutron scattering experiments. The intra-layer exchange only weakly changed with doping while the inter-layer one drastically decreased. Here we propose a theory which accounts for these experimental findings. We argue, that the observed striking doping dependence of the exchange energies can be attributed to the evaluation of the orbital level splitting with doping. The latter is handled by the interplay between Jahn-Teller effect (supporting an axial orbital) and the orbital anisotropy of the electronic band in the bilayer structure (promoting an in-plane orbital), which is monitored by the Coulomb repulsion. The presented theory, while being a mean-field type, describes well the experimental data and also gives the estimates of the several interesting energy scales involved in the problem.

PACS numbers: 75.30.Ds, 75.10.Lp, 75.30.Vn

The three-dimensional (3D) cubic manganites $\text{R}_{1-x}\text{B}_x\text{MnO}_3$ (where R is trivalent rare-earth and B is divalent alkaline ion, respectively) as well as the two-dimensional (2D) bilayer ones $\text{La}_{2-2x}\text{Sr}_{1+2x}\text{Mn}_2\text{O}_7$ have attracted recent interest not only due to the discovery of colossal magnetoresistance (CMR) in these compounds but also because of their rich and rather unusual physical properties.¹ At different doping concentration the manganese oxides exhibit a wide diversity of the ground states, and the small changes of some external parameters of the system such as doping, chemical pressure, temperature or magnetic field can result in a drastic modification of the physical properties as well as cause the transition from one to another ground state.

In fact, in very recent spin-wave measurements on the bilayer manganites $\text{La}_{2-2x}\text{Sr}_{1+2x}\text{Mn}_2\text{O}_7$ (in the doping range $x = 0.3 - 0.5$) strongly anisotropic doping dependence of the inter-layer (within the bilayer) (J_{\perp}) and of the intra-layer (J_{\parallel}) exchange couplings has been revealed.^{2,3} At $x = 0.3$ both exchange constants are ferromagnetic (FM) and of the same order $J_{\perp} = 5$ meV, and $J_{\parallel} = 4$ meV.² With further doping ($x > 0.3$), J_{\parallel} changes very slightly while inter-layer exchange rapidly decreases, by a factor of four at $x = 0.4$, and changes sign at $x \sim 0.45$.

Within the double-exchange (DE) picture FM coupling between the nearest-neighbour (NN) t_{2g} core spins is mediated by the hopping of e_g -electrons ($d_{x^2-y^2}$ and $d_{3z^2-r^2}$ orbital states) and scales as a kinetic energy of these electrons on a given bond. Since only $d_{3z^2-r^2}$ (axial) orbital has a finite inter-layer transfer amplitude (z -axes is set perpendicular to a bilayer), the inter-layer exchange is *only* mediated by this orbital. While the intra-layer one is *mainly* determined by the $d_{x^2-y^2}$ (in-plane) orbital state, that has a highest intra-plane transfer amplitude. Therefore, above discussed decrease of

the inter-layer exchange constant with doping can be ascribed to the change of the nature of occupied orbital state from mainly $d_{3z^2-r^2}$ character, at low doping $x < 0.3$, to mostly $d_{3z^2-r^2}$ one at higher doping.^{2,3} This qualitative picture is also consistent with the recent x-ray magnetic Compton-profile measurements.⁴ The results of this experiment have shown that upon doping (for $0.35 < x < 0.45$) the electrons are mainly withdrawn from $d_{3z^2-r^2}$ orbital state and the occupancy of $d_{x^2-y^2}$ state remains practically the same. However, we point out, that the observed doping dependence of the exchange constants and of the orbital occupancy, being interrelated, can not be understood within a rigid band picture that assumes a constant value of orbital level splitting. Interpretation of the experimental findings within this picture would imply that only $d_{3z^2-r^2}$ band crosses the Fermi level and is emptied out upon doping, while the $d_{x^2-y^2}$ band lies below and shows a constant filling. From the other hand, if $d_{x^2-y^2}$ band does not cross Fermi surface, then it is no longer active to generate the intra-layer ferromagnetic DE interaction leading to $J_{\parallel} < J_{\perp}$, in contrast to experimental findings $J_{\parallel} > J_{\perp}$.

The aim of the present work is to propose a mechanism that can explain the experimental findings. The paper is organized as follows: First we briefly discuss the structural aspects of the compound relevant for our study. Next we give the basic physical ideas and set up the minimal model Hamiltonian to provide a microscopic description. We then present our results on the doping evaluation of the orbital occupancies and the exchange energies, and finally, compare the theoretical findings with that of the experiments.

The compound $\text{La}_{2-2x}\text{Sr}_{1+2x}\text{Mn}_2\text{O}_7$ consists of bilayer slices of MnO_6 octahedra, separated by insulating $(\text{La},\text{Sr})_2\text{O}_2$ layers that serve to decouple the bilayers both electronically and magnetically. Therefore, as a first ap-

proximation the system can be treated as composed of independent bilayers. One electron placed in the doubly degenerate e_g level, makes the $\text{Mn}^{+3}\text{O}_6^{-2}$ complex Jahn-Teller (JT) active. The experimental analysis of the crystal structure has revealed, that JT distortion results in the elongation of MnO_6 octahedra along z -axis.⁵ Five bonds (four equatorial and one apical with shared oxygen ion) are essentially identical. The elongation of octahedra occurs mainly because the apical bond with unshared oxygen atom is longer than the other five bonds. These type of JT distortion promotes the axially directed $d_{3z^2-r^2}$ orbital by lowering its on-site energy. The dimensionless parameter describing the static Jahn-Teller distortion can be defined as $\delta_{\text{JT}} \equiv (\langle d_{\text{Mn-O}}^{\text{apic}} \rangle - \langle d_{\text{Mn-O}}^{\text{equat}} \rangle) / \langle d_{\text{Mn-O}}^{\text{equat}} \rangle$, where $\langle d_{\text{Mn-O}}^{\text{apic(equat)}} \rangle$ is an averaged apical (equatorial) Mn-O length. The relative distortion δ_{JT} also gives the scale of JT induced orbital level splitting.

The physical picture we shall be based on is as follows: Both the orbital occupancy and exchange energies strongly depend on the orbital level splitting. The latter consist of the two parts: JT induced gap and correlation induced one. The JT distortion is largest at low doping and monotonically relaxes upon doping ($\delta_{\text{JT}} \sim 0.036, 0.020$, and 0.0 for $x = 0.3, 0.4$, and 0.5 , respectively).⁵ Therefore, at low doping the axial orbital, promoted by the JT distortion is predominantly occupied. The matrix element of the inter-orbital Coulomb energy does not depend on the character of predominantly occupied orbital state. Therefore, on-site repulsion further supports already preferred orbital state and by enhancing the orbital polarization reduces the Coulomb energy.⁶ At low doping, the physics is mainly determined locally and kinetic energy term is less important. However, upon increasing the carriers number the JT induced gap decreases while the kinetic energy starts to play more dominant role. In the bilayer system, the latter promotes the in-plane orbital state, that has the highest intra-layer transfer amplitude and by forming the wider band can lower the kinetic energy of the system. Therefore, one would expect that at some doping $x = x_c$ the possible energy gain due to the kinetic energy will overcome the crystal-field splitting of the orbital levels. Therefore, for $x > x_c$, it becomes energetically more favorable to lower the energy of the in-plane orbital and hence, correlation induced splitting will change the sign. As will be shown below, the doping dependence of the orbital level splitting, resulted from the discussed interplay, gives the consistent description of the experimental findings.

The minimal model Hamiltonian which describes above discussed scenario consists of the two contributions $H = H_{\text{el}} + H_{\text{sp}}$, where H_{el} and H_{sp} describe charge and spin degrees of freedom, respectively.⁷ Retaining only the preferred spin component of the fermionic operators, in the fully polarized (semi-metallic) FM case the electronic part of the Hamiltonian can be written as:

$$\begin{aligned}
H_{\text{el}} = & - \sum_{ij,\alpha,\beta} t_{\parallel,ij}^{\alpha\beta} \left[d_{i\alpha}^\dagger d_{j\beta} + \bar{d}_{i\alpha}^\dagger \bar{d}_{j\beta} \right] \\
& - \sum_{i,\alpha,\beta} t_{\perp}^{\alpha\beta} \left[d_{i\alpha}^\dagger \bar{d}_{i\beta} + \text{H.c.} \right] \\
& + \sum_{i,\alpha} [(-1)^\alpha \Delta_{\text{JT}} - \mu] [n_{i\alpha} + \bar{n}_{i\alpha}] \\
& + \sum_{i,\alpha \neq \beta} U [n_{i\alpha} n_{i\beta} + \bar{n}_{i\alpha} \bar{n}_{i\beta}] \quad (1)
\end{aligned}$$

The first and the second term of Eq.(1) describe an intra- and inter-layer electron hopping between the two e_g orbitals of the NN Mn-ions, respectively. Index i numbers the unit cell composed by two Mn sites, $d_{i\alpha}$ and $\bar{d}_{i\alpha}$ are the electron annihilation operators on these two sites. The orbitals $d_{3z^2-r^2}$ and $d_{x^2-y^2}$ correspond to $\alpha(\beta) = 1$ and 2 , respectively. Intra- and inter-layer transfer matrix elements are given by

$$t_{\parallel,x(y)}^{\alpha\beta} = t \begin{pmatrix} 1/4 & \mp \sqrt{3}/4 \\ \mp \sqrt{3}/4 & 3/4 \end{pmatrix}, \quad t_{\perp}^{\alpha\beta} = t \begin{pmatrix} 1 & 0 \\ 0 & 0 \end{pmatrix} \quad (2)$$

The electron density operator on a given orbital state is denoted by $n_{i\alpha}$, μ is chemical potential, $\Delta_{\text{JT}} = g\delta_{\text{JT}}$ is JT induced orbital level splitting, g is properly normalized coupling constant of electrons with JT active phonon modes, and δ_{JT} is a measure of JT distortion discussed above. In the present paper we do not attempt to calculate JT distortion by minimizing the total energy of the system (including lattice elastic energy) and model the dimensionless parameter δ_{JT} by the following doping dependence $\delta_{\text{JT}} = 0.17(0.5-x)$, that reasonably reproduces the experimental data.⁵

The last term in Eq.(1) represents the on-site inter-orbital Coulomb repulsion U between electrons. We treat this term within the mean-field (MF) approximation by introducing the MF parameter describing the anisotropy of the orbital occupancy $\delta n = \langle n_1 \rangle - \langle n_2 \rangle$. This introduces additional splitting of local orbital levels due to the electron correlations. Therefore the total splitting of orbital levels will be determined by both JT and correlation effects with following value: $2\Delta = 2\Delta_{\text{JT}} + U\delta n$. We would like to emphasize that the nonzero value of MF parameter δn does not imply any symmetry breaking long range orbital order and the symmetry of Hamiltonian remains tetragonal. Even in the non-interacting case and absence of any JT distortion one finds $\delta n \neq 0$. The band structure with tetragonal symmetry brakes the local cubic symmetry and promotes planar $d_{x^2-y^2}$ orbital with wider band leading to $\delta n < 0$. In the orbital pseudo-spin language the ground state can be represented by nonzero value of the axial component of the orbital pseudo-spin $\langle \tau_i^z \rangle = \langle (n_{i1} - n_{i2})/2 \rangle \neq 0$ due to the nonzero pseudo-magnetic field produced by the 2D structure of the system, and with no order in the pseudo-spin basal plane $\langle \tau_i^{x(y)} \rangle = 0$.

The resulted MF Hamiltonian is bilinear and can be diagonalized by two subsequent canonical

transformations.⁸ First step is to introduce the bonding and anti-bonding states as $a(b)_{\alpha(\beta)\mathbf{k}} = [d_{\alpha(\beta)\mathbf{k}} \mp \bar{d}_{\alpha(\beta)\mathbf{k}}]/\sqrt{2}$ and decouple the MF Hamiltonian in two parts each consisting of the two orbitals. The next transformation

$$\begin{cases} A(B)_{1\mathbf{k}} = u_{\mathbf{k}}^{a(b)} a(b)_{1\mathbf{k}} + v_{\mathbf{k}}^{a(b)} a(b)_{2\mathbf{k}} \\ A(B)_{2\mathbf{k}} = -v_{\mathbf{k}}^{a(b)} a(b)_{1\mathbf{k}} + u_{\mathbf{k}}^{a(b)} a(b)_{2\mathbf{k}} \end{cases} \quad (3)$$

diagonalizes the two-band Hamiltonian bringing it into the form:

$$H = \sum_{\mathbf{k}\alpha} \left[\varepsilon_{\alpha\mathbf{k}}^a A_{\alpha\mathbf{k}}^\dagger A_{\alpha\mathbf{k}} + \varepsilon_{\alpha\mathbf{k}}^b B_{\alpha\mathbf{k}}^\dagger B_{\alpha\mathbf{k}} \right]. \quad (4)$$

The coherence factors and eigen-frequencies are given by

$$u[v]_{\mathbf{k}}^{a(b)} = [\text{sgn}(\varepsilon_{\mathbf{k}}^{12})] \frac{1}{\sqrt{2}} \left[1 + [-] \frac{\varepsilon_{a(b)\mathbf{k}}^{11} - \varepsilon_{\mathbf{k}}^{22}}{\varepsilon_{1\mathbf{k}}^{a(b)} - \varepsilon_{2\mathbf{k}}^{a(b)}} \right]^{\frac{1}{2}},$$

$$\varepsilon_{1(2)\mathbf{k}}^{a(b)} = \frac{\varepsilon_{a(b)\mathbf{k}}^{11} + \varepsilon_{\mathbf{k}}^{22}}{2} \pm \sqrt{\frac{[\varepsilon_{a(b)\mathbf{k}}^{11} - \varepsilon_{\mathbf{k}}^{22}]^2}{4} + [\varepsilon_{\mathbf{k}}^{12}]^2} \quad (5)$$

with the following notations $\varepsilon_{a(b)\mathbf{k}}^{11} = -t\gamma_{\mathbf{k}} \pm t - \mu + \Delta$, $\varepsilon_{\mathbf{k}}^{22} = -3t\gamma_{\mathbf{k}} - \mu - \Delta$, $\varepsilon_{\mathbf{k}}^{12} = -\sqrt{3}t\bar{\gamma}_{\mathbf{k}}$, and $\gamma(\bar{\gamma})_{\mathbf{k}} = [\cos k_x \pm \cos k_y]/2$.

The above introduced MF parameter δn and chemical potential μ for a given doping can be obtained from the system of self-consistent equations which in terms of the obtained eigen-states (3-5) of MF Hamiltonian reads as:

$$n = \frac{1}{2N} \sum_{\mathbf{k}} \{n(\varepsilon_{1\mathbf{k}}^a) + n(\varepsilon_{2\mathbf{k}}^a) + [b \rightarrow a]\} \quad (6)$$

$$\delta n = \frac{1}{2N} \sum_{\mathbf{k}} \{[(1 - 2(v_{\mathbf{k}}^a)^2)[n(\varepsilon_{1\mathbf{k}}^a) - n(\varepsilon_{2\mathbf{k}}^a)] + [b \rightarrow a]\}$$

where $n(\varepsilon)$ is the Fermi distribution function.

Lets us now discuss the spin degrees of freedom of the system. In the DE exchange limit (Hund's coupling $J_{\text{H}} \gg W$ carriers band-width) the spin subsystem in the two orbital model can be also mapped to an effective NN Heisenberg model

$$H = - \sum_{i,\delta_{\parallel}} J_{\parallel} \mathbf{S}_i \mathbf{S}_{i+\delta_{\parallel}} - \sum_{i,\delta_{\perp}} J_{\perp} \mathbf{S}_i \mathbf{S}_{i+\delta_{\perp}} \quad (7)$$

with effective intra-layer J_{\parallel} and inter-layer J_{\perp} FM exchange couplings defined as $J_{\parallel} = J_{\parallel}^{DE} - J$, $J_{\perp} = J_{\perp}^{DE} - J$, and J is the antiferromagnetic super-exchange constant between the t_{2g} spins. Ferromagnetic intra- and inter-layer DE energies are given by

$$J_{\parallel}^{DE} = \sum_{\alpha,\beta} t_{\parallel}^{\alpha\beta} \frac{\langle d_{i,\alpha}^\dagger d_{j,\beta} \rangle}{2S^2}, \quad J_{\perp}^{DE} = \sum_{\alpha,\beta} t_{\perp}^{\alpha\beta} \frac{\langle d_{i,\alpha}^\dagger \bar{d}_{j,\beta} \rangle}{2S^2}. \quad (8)$$

With the above formulated scheme we proceed as follows. First, we solve the MF equations (6) to determine,

the orbital level splitting Δ and chemical potential μ for a given doping. Then, expressing the Eq. 8 for the exchange constants in terms of the eigen-states of the MF Hamiltonian we end up with the intra- and inter-layer exchange energies for a given doping. Model parameters are fixed in a way to reproduce the experimental results.

In Fig. 1 the calculated doping dependence of intra- and inter-layer exchange couplings is presented together with the experimental data from Refs. 2,3,9 (see also Ref. 10). The best fit to the data has been achieved for the following values of the model parameters: $t = 0.18$ eV, $U = 0.7$ eV, $g = 0.5$ eV, and $2SJ = 11$ meV (see also discussion below). The hopping integral sets the overall energy scale. The value of JT splitting, hence of electron-phonon coupling strength fixes the doping at which $J_{\parallel} = J_{\perp}$ and system shows the isotropic behavior. The Coulomb U determines the steepness of the drop of inter-plane exchange constants and the AFM superexchange J shifts the whole picture rigidly relative to the Y axis of Fig. 1. Therefore, despite the number of independent parameters all of them can be unambiguously extracted from the fitting.

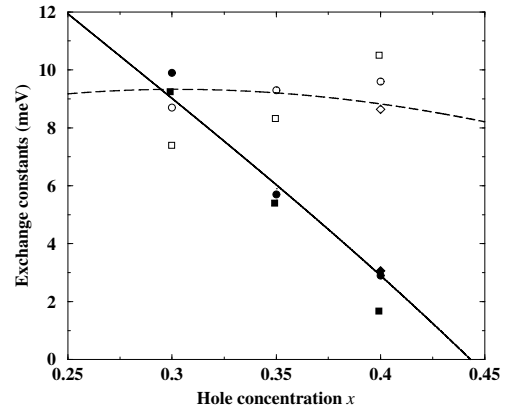


FIG. 1. Inter- (SJ_{\perp}) and intra-layer (SJ_{\parallel}) exchange constants as a function of hole concentration (solid and dashed line, respectively). The filled (open) circles, squares, and diamonds are inter-(intra-)layer exchange constants from neutron scattering data of Refs. 2, 3, and 9, respectively.

As it is seen from Fig. 1 the intra-layer exchange is practically unaffected by doping while the inter-layer one is dramatically reduced. When inequality $J_{\perp}^{DE} < J$ becomes valid, the antiferromagnetic super exchange prevail ferromagnetic DE signaling the instability of the FM ground state of the bilayer. In fact, neutron diffraction study on $x = 0.5$ sample revealed the A-type AFM ordering.⁵

As it follows, the above discussed doping dependence of the exchange constants is in one to one correspondence with the doping dependence of the orbital occupancy. The latter is shown in Fig. 2 calculated for the same values of the model parameters. The experimental data from Ref. 4 is also presented on the same plot.

The in-plane $d_{x^2-y^2}$ orbital (dashed line in Fig. 2) is predominantly occupied and shows weak doping dependence in almost whole presented range of the hole concentration. While axially directed $d_{3z^2-r^2}$ orbital (solid line in Fig. 2) is emptied-out linearly with doping, i.e. all the doped hole in this doping range resides on $d_{3z^2-r^2}$ orbital. The value of JT induced gap determines the doping x_c , at which $\delta n = 0$ and both orbitals are equally populated. Coulomb repulsion U is responsible for the steepness of the drop of $d_{3z^2-r^2}$ level occupancy.

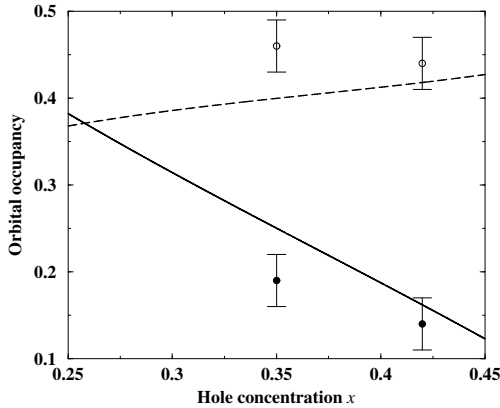


FIG. 2. Occupancy of $d_{3z^2-r^2}$ (solid line) and $d_{x^2-y^2}$ (dashed line) orbitals as a function of hole concentration. The open (filled) circles are the experimental data for $d_{x^2-y^2}$ ($d_{3z^2-r^2}$) orbital occupancy from Ref. 4.

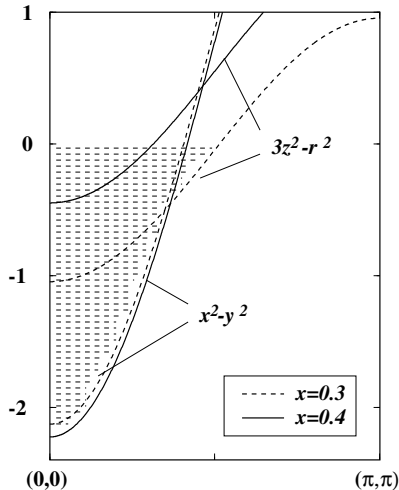


FIG. 3. Bonding $3z^2-r^2$ and x^2-y^2 bands (in units $t = 1$) referred to chemical potential for hole doping $x = 0.3$ (dashed line) and $x = 0.4$ (solid line).

The above discussed evaluation of the orbital occupancy upon doping can be understood as follows. In the doping range $x < x_c$, ($x_c \simeq 0.26$ being the hole concentration at which both orbitals are equally occupied [see Fig. 2]) the JT distortion is large and stabilizes the axially directed orbital. With doping JT induced gap weakens and at $x = x_c$ the kinetic energy term supporting the

in-plane orbital state takes over. Therefore, δn changes sign at $x = x_c$ and the $d_{x^2-y^2}$ orbital starts to be predominantly populated. For $x > x_c$ correlation induced splitting $2\Delta_{cor} = U\delta n$ is negative and supports in-plane orbital. With farther doping, the orbital anisotropy δn increases, leading to increase of correlation induced splitting. Therefore, the axial band is pushed up relative to the in-plane band upon doping, while the chemical potential is practically pinned. Therefore, all the doped holes go to the upper $d_{3z^2-r^2}$ band and its occupancy linearly decrease upon doping, while the population of lower $d_{x^2-y^2}$ band is only weakly changed.

This doping dependence of the band structure is explicitly shown in Fig. 3, where the bonding $d_{x^2-y^2}$ and $d_{3z^2-r^2}$ bands are presented for hole concentration $x = 0.3$ (dashed line) and $x = 0.4$ (solid line).

Let us now discuss the model parameters used to reproduce the experimental data. The value of the hopping integral $t = 0.18$ eV is in the range estimated for manganese oxides $t \simeq 0.1 \sim 0.3$ eV. Moderate value of the inter-orbital Coulomb repulsion $U = 0.7$ eV is sufficient to give reasonable fit to the data, which justifies the MF treatment adopted here. The AFM superexchange energy of t_{2g} spins remarkably coincides with one ($2SJ = 10$ meV) estimated from the spin-wave data of $\text{Nd}_{0.45}\text{Sr}_{0.55}\text{MnO}_3$.⁸ Another important parameter is the JT splitting of the orbital states, that is difficult to directly detected experimentally. For $x = 0.3$, with the above estimate of the electron-phonon coupling constant one obtained the JT splitting $2\Delta_{JT} \simeq 0.035$ eV. Hence, in the doping regime considered here, the JT binding energy is much smaller than the carriers band-width. This explains why the polaronic effects, not considered in the present paper, can be ignored.

The authors would like to thank T. Chatterji, N. M. Plakida, V. Yu. Yushankhai and M. E. Zhitomirsky for useful discussions. G. J. acknowledges support from a *Bourse Post-Doctoral du ministère de l'Education nationale, de la recherche et de la technologie* and N. B. P. acknowledges support from the Visitor Program of MPI-PKS, Dresden. The partial support by INTAS program, Grant No. 97-11066, is also acknowledged.

* On leave from E. Andronikashvili Institute of Physics, Georgian Academy of Sciences, Tbilisi, Georgia.

¹ For a review, see, for example, E. Dagotto, T. Hotta and A. Moreo, Phys. Rep. **344**, 1 (2001); E.L. Nagaev, *ibid.* **346**, 387 (2001).

² K. Hirota, S. Ishihara, H. Fujioka, M. Kubota, H. Yoshizawa, Y. Morimoto, Y. Endoh, and S. Maekawa, cond-mat/0104535 (unpublished).

³ T.G.Perring, D.T. Adroja, G. Chaboussant, G. Aeppli, T. Kimura, and Y. Tokura, cond-mat/0105230 (to be pub-

lished in Phys. Rev. Lett.).

⁴ A. Koizumi, S.Miyaki, Y. Kakutani, H. Koizumi, N. Hiraoka, K. Makoshi, and N. Sakai, K. Hirota, and Y. Murakami, Phys. Rev. Lett. **86**, 5589 (2001).

⁵ M. Kubota, H. Fujioka, K. Hirota, K. Ohoyama, Y. Moritomo, H. Yoshizawa, and Y. Endoh, J. Phys. Soc. Jpn. **69**, 1606 (2000).

⁶ In the fully polarized ferromagnetic phase, considered here, the role of intra-orbital Coulomb repulsion is insignificant and can be dropped out.

⁷ Since in the present work only the the effect of orbital degree's of freedom on the exchange coupling is considered, the term describing the interaction between the spin and charge degrees of freedom is dropped out from the model

Hamiltonian.

⁸ G. Jackeli, N. B. Perkins and N. M. Plakida, Phys. Rev. B **62**, 372 (2000); **64**, 092403 (2001).

⁹ T. Chatterji, L. P. Regnault, P.Thalmeier, R. Suryanarayanan, G. Dhahlenne, and A. Revcolevschi, Phys. Rev. B **60**, R6965 (1999).

¹⁰ The slight discrepancy between the values of the intra-layer exchange reported by the various experimental groups is probably due to the fact, that the different momentum regions of the spin-wave spectra have been used by those groups to extract J_{\parallel} . The inter-layer exchange can be more accurately determined, since it sets the momentum independent splitting of bonding and anti-bonding spin-wave spectra.